Development of Bed Ridges in Open Channels and their Effects on Secondary Currents and Wall Shear

KAMRAN ANSARI*, ASHFAQUE AHMED MEMON*, AND NAEEM AZIZ MEMON**

RECIVED ON 08.02.2012 ACCEPTED ON 21.06.2012

ABSTRACT

A numerical analysis of the ridges on the bed of wide, open channels and their effects on the distribution of secondary currents and wall shear is undertaken using CFD (Computational Fluid Dynamics). The presence of the lines of boil, consisting of low speed streaks, periodically in the transverse direction, is reported in the literature due to the presence of the ridges. In the present work, simulations are run on channel sections with varying the number of ridges on the bed and the size of these ridges. The effect of these variations on the flow structures and shear stress distribution in wide open channels is reported. The results offer an interesting insight into the 3D (Three-Dimensional flow structures involved and the link between flow structures and bed morpho-dynamics in prismatic channels.

Key Words: **Open Channels, CFD Modelling, Ridges, Boundary Shear Stress, Secondary Currents.**

1. INTRODUCTION

The study of the cellular secondary currents in open channel hydraulics is very important as they are responsible for the 3D nature of flow patterns, and determine wall shear stress distributions, sediment transport and bed forms [1]. Open channel flows are mostly complex and the along channel flow, is greatly affected by the secondary flow in the cross stream and vertical directions. Prandtl [2] classified secondary flows into two categories. Secondary flow of first kind is usually seen in curved or meandering channels in which the flow may circulate in the cross-sectional plane either driven by centrifugal or transverse pressure gradients. Secondary flow of the second kind is related to the non-homogeneity and anisotropy of the turbulence and may be caused due to number of reasons such as asymmetry of the channel boundaries, free surface effects or variation in bed conditions [3-4].

So-called lines of boil, consisting of low speed streaks, which are high in sediment load, have been reported in the river flow literature. These boiling streets, as they are usually known, are formed periodically in the channel transverse direction and the distance between any two neighbouring boiling lines is around twice the flow depth [5]. Some experimental research work has been carried out, following on from field observations, on the fluid motion in conduits with longitudinal bed forms. Nezu, et. al. [6] carried out some experimental preliminary work on cellular secondary currents to assess the interaction between secondary currents and the bed forms. Using LDA (Laser Doppler Anemometer) and ultra sonic bed form instrument Nezu, et. al. [7-8] found that some organized fluid motions and the associated sediment transport occurred side by side on a moveable plane sand bed.

* Assistant Professor, and ** Lecturer,
Department of Civil Engineering, Mehran University of Engineering & Technology Jamshoro.

Nezu, et. al. [6- 9] proposed that the evolution process of longitudinal bed forms starts with the presence of the corner vortex which is created due to the sidewall effect. This corner vortex creates lateral variations in bed shear stress and ultimately leads to the formation of the sand ridges near the walls. This further modifies the bed shear stress in the lateral direction, generating new vortices. This process carries on until the cellular secondary currents and the sand ridges occur across the entire section and an equilibrium state is reached. Colombini [10] however, argues that the initiation of cellular secondary flows is an instability-related process. Small disturbances either from the bed surface or the flow itself are responsible for the stream-wise vortices which then produce lateral sediment transport and sorting. Nezu, et. al. [1] also point out that when aspect ratio, b/h, where b and h are the channel width and depth respectively, is greater than or equal to 5, the time averaged secondary currents are not readily identified, but instantaneous patterns do exist. They fluctuate in time and space and might disappear in a time-averaged analysis. These instantaneous secondary currents may be responsible for the formation of smooth and rough strips on the bed and, ultimately, sand ribbons, which in turn stabilize secondary currents in space.

Ikeda [11] studied the size and shape of the self formed strips with uniform non-cohesive sands and found that longitudinal sand ridges were formed over the entire movable bed. The crests of the ridges were several millimetres high and the distance between adjacent crests was roughly twice the flow depth.

Nezu, et al. [12] mention that the bed shear stress attains a mild peak in the side-wall zone and would be scoured first to become a trough. This sand thus scoured would be carried both downstream because of the downstream velocity component, u, and sideways because of the lateral velocity component, v, (corner cellular currents) and then gather to form the first ridge.

Ansari, et. al. [13] have studied the wall shear and secondary current variation in trapezoidal channels and also found that no secondary currents were generated in the central portion of the wide channels (b/h>5) with rigid beds. They were initially concerned that their model was incomplete, though it agreed with Nezu, et. al. [1], but decided to investigate this issue further. The detailed mechanisms that control the generation and maintenance of cellular secondary currents (and the resulting bed forms) have not yet been explained [14]. It is the mutual interaction between morpho-dynamics and hydrodynamics that is responsible for the bed ridges and the boiling streets. This study is therefore, focused on the 3D steady flow structures created in the central portion of wide channels after the formation of ridges on the bed. These areas are known to have purely 2D flow in the absence of these longitudinal bed forms. A fixed bed has been used in the simulations and the ridges have been artificially added sequentially on the bed, from the outside to the inside, to simulate the formation of longitudinal ridges and troughs along the bed.

2. GEOMETRY USED

The channels sections are 900mm wide at the bed and have a fixed depth of water of 80mm. With reference to Fig. 1, the channels have three different cross sections of ridges fixed on their bed and have been named accordingly e.g. Case 75-10-6 means the width of the ridge, b_1, is 75mm, the height of the ridge, h_1, is 10mm and the number of ridges on bed are 6. The centre to centre distance between two adjacent ridges, λ, is fixed as 150 mm which is nearly equal to twice the depth of water in the channel. The first ridges near the sidewalls are fixed at a distance of $\lambda/2$. The cross section has been divided into sections and numbered from left wall, odd numbers being the troughs and even numbers being the ridges, as shown in Fig. 1.

3. NUMERICAL MODELLING

The commercially available CFD software ANSYS-CFX Version 11 [15] was used.

3.1 Governing Equations

The numerical modelling involves the solution of the so-called RANS (Reynolds Averaged Navier Stokes) equations can be written in tensor form as, first, for the continuity equation:

$$\frac{\partial \rho}{\partial t} + \frac{\partial}{\partial x_i}\left(\rho U_i\right) = 0 \tag{1}$$

where ρ is the density, U_i are the mean components of velocity and second, for the conservation of momentum.

$$\frac{\partial}{\partial t}\left(\rho U_i\right) + \frac{\partial}{\partial x_j}\left(\rho U_i U_j\right) = -\frac{\partial P}{\partial x_i} + \frac{\partial}{\partial x_i}\left[\mu\left(+\frac{\partial U_i}{\partial x_i} + + \frac{\partial U_i}{\partial x_i}\right)\right] + \frac{\partial}{\partial x_i}\left(-\rho\overline{u_i' u_j'}\right) \tag{2}$$

where P is the mean pressure, u_i' is the fluctuating part of the velocity and μ is the dynamic viscosity. The terms $-\rho\overline{u_i' u_j'}$ in Equation (2) are referred to as the Reynolds Stresses and represent six additional unknowns in the RANS equations that must be modelled or resolved in some way to allow for the solution of Equations (1-2). Conceptually the simplest such model, and the most accurate for the physics involved in straight prismatic channels due to anisotropic effects [16], provides one equation for each Reynolds stress as well as one equation for the dissipation of turbulence energy. A large number of turbulence models are available to this effect and in particular the Launder, et. al. [17], or LRR, and the Speziale, et. al. [18], or SSG, models. The SSG model was chosen here following on from the works of Cacqueray, et. al. [19] and in Ansari, et. al. [13] respectively. A standard wall function is used to calculate the wall effect on the solution at the wall-adjacent node. The SSG model presents an advantage over the more classic Launder, et. al. [17] model in that it uses a quadratic relationship for the pressure redistribution and does not require any additional term to account for the wall effects, which is numerically difficult to implement. Its usage has also grown considerably and it is now a well established model.

3.2 Boundary Conditions and Coordinate System

A consistent frame of reference for the coordinate axes is taken with the x-axis corresponding to the stream-wise direction, the y-axis to the cross stream direction and the z-axis to the vertical direction. The three components of velocity u,v, and w are aligned with the axes x-, y- and z-axes respectively. The origin is placed at the left most part of the channels and coincides with the base of the channel and the water is taken to be flowing in the positive x-direction. Both the walls (bed and side) were taken as non-slip smooth walls. The free surface was modelled using a symmetry boundary condition. All the simulations were solved as single phase, steady state problems with

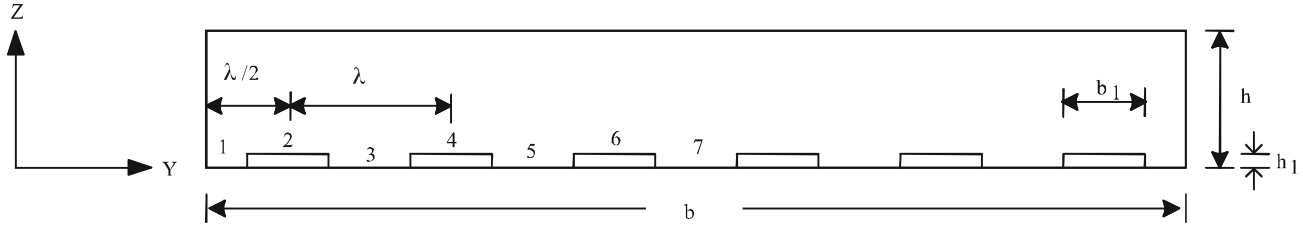

FIG. 1. TYPICAL CROSS SECTION OF THE CHANNEL WITH BED FORMS

water used as the fluid. Periodic boundary conditions were used on the up- and downstream faces of the single cell thick section, hence a momentum source in the stream-wise equal to ρgS, where ρ is the density of water (997 kg/m^3), g is the acceleration due to gravity (9.81 m/s) and S is the slope of the channel (0.0006 m/m), was applied. As a consequence of using periodic boundary conditions a cycle was created which drives the flow of water until it reaches a steady state condition (defined in Section 3.4).

3.3 Mesh Generation

The domain is meshed entirely using hexahedral cells. A mesh of uniform cell size i.e. uniform cell height (z-direction) and uniform width (y-direction) was built. Keeping the mesh uniform helps in reducing the variations obtained in the values of y^+ when adding the ridges. The y^+ values found for the simulations vary typically between 15 and 25. The number of cells in the cross section varied between 67,580 and 72,000.

3.4 Convergence Criteria

For steady-state problems in CFX, a time scale (pseudo time step) is used as an "acceleration parameter" to guide the solution process. Here the time scale was 0.1 second. All the non-dimensionalized residual targets were set at 10^{-9}. It was found necessary to use such low targets to ensure that the shear forces on the bed and sidewall reached steady values and matched the applied body force. Such tight convergence criteria were required because the secondary currents took a great number of iterations to establish themselves in the first place.

4. RESULTS

4.1 Validation of the Model Used

Before the start of the actual study one simulation was run on the channel section used by Nezu, et. al. [5] during their experimental work. The purpose of this simulation was to verify the prediction of re-circulations obtained in the cross-section of the channel section due to the presence of ridges on the beds. The channel section used was called Case-J during the experimental study. The channel dimensions and hydraulic conditions can be found in detail in Nezu, et. al. [5].

Fig. 2(a) shows the flow pattern of cellular secondary currents of Case-J as measured by Nezu, et. al. [5] during their experimental study and Fig. 2(b) show the flow pattern of cellular secondary currents as predicted by CFD simulation. The results are very encouraging as CFD simulations are able to predict accurately the flow pattern of the secondary currents. The validation of the numerical model is also done extensively in the previous works of the authors' (Cacqueray, et. al. [19] and Ansari, et. al. [13]).

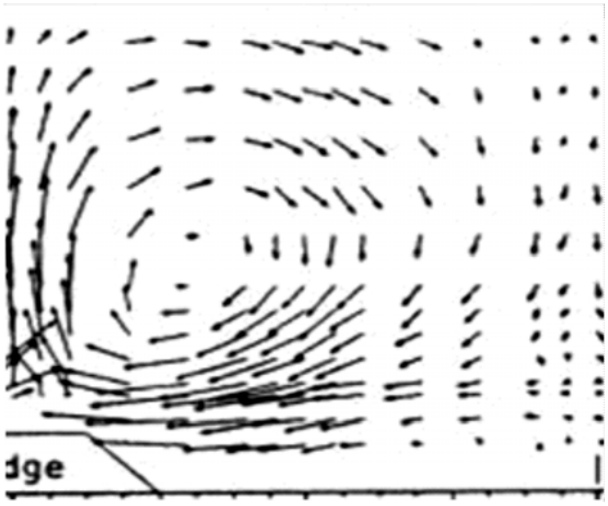

(a) EXPERIMENTAL

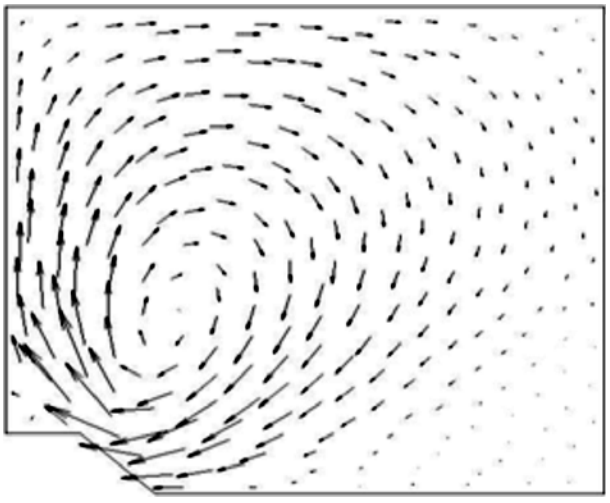

(b) CFD

FIG. 2. FLOW PATTERN OF CELLULAR SECONDARY CURRENTS (CASE-J) NEZU, ET. AL. [6]

The results of six channel geometries are presented next, with two types of variations being performed i.e. (i) number of ridges, and (ii) size of the ridges, on the bed. The six cases are named according to the size and number of ridges as discussed in Section 2 above. The flow characteristics of all the six cases are given in Table 1. Some of the results based on CFD simulations are discussed below.

4.2 Initiation of Ridges

The secondary currents and wall shear are plotted to assess whether the presence of secondary currents is a possible mechanism for the initiation of ridges on the bed.

4.2 Initiation of Cellular Secondary Currents

Fig. 3 shows secondary currents plots for the four cases with variation in the number of ridges on the bed i.e. a channel with no ridge on the bed (Case 75-10-0), a channel with two ridges near the sidewalls (Case 75-10-2) and then a channel with two (Case 75-10-4) and four (Case 75-10-6) additional ridges towards the middle portion. The channel without any ridge on the bed shows a strong cellular flow only near the wall as a result of the local unbalance in the Reynolds stresses. Away from the wall towards the central portion, the currents reduce in strength and, in fact, virtually vanish, as shown in Fig. 3(a). This strong circulation near the sidewalls on the other hand could well be responsible for the initiation of the sand ridges on the bed, as hypothesized by others, e.g. Nezu, et. al. [5].

In Fig. 3(b) an additional vortex appears as soon as the two ridges near the sidewalls are added. The secondary currents in the area just after the ridges become stronger due to the presence of the ridges, which, again and in turn, could be arguably responsible for the creation of additional ridges towards the central portion of the channel leading to Fig. 3(c-d).

Fig. 4 shows the velocity component, v, in the transverse (y-axis) direction, near the bed at four different sections for four Cases 75-10-0, 75-10-2, 75-10-4 and 75-10-6. The graph shows that velocity v is continuously increasing in Region 1 (location defined in Fig. 1), when there is no ridge, and may be responsible for the creation of the corner ridge. Just after the formation of the first corner ridge the transverse velocity is seen to stabilise and little variation is observed. At Location 3, which immediately follows the corner ridge, the cross stream velocity is seen to be continuously decreasing when there are no ridges. The appearance of the first corner ridge leads to a second large peak in velocity. This increase in velocity could in turn be responsible for the creation of an additional ridge towards the centre of the channel. Similar results are seen at Locations 5 and 7 where the cross stream velocity is seen to increase as a result of the creation of new ridges.

TABLE 1. FLOW CHARACTERISTICS OF CHANNELS.

Case Number	Discharge (Q)	Mean Velocity (U_m)	Maximum Velocity (U_{max})	Reynolds Number (R_e)	Froude Number (F_r)
	($m^3.s^{-1}$)	($m^3.s^{-1}$)	($m^3.s^{-1}$)		
75-10-0	0.0322	0.446	0.524	135684	0.50
75-10-2	0.0309	0.437	0.522	125440	0.49
75-10-4	0.0293	0.423	0.514	114809	0.48
75-10-6	0.0277	0.408	0.485	104712	0.46
75-05-6	0.0300	0.428	0.506	119484	0.48
]50-10-6	0.0287	0.414	0.492	108517	0.47

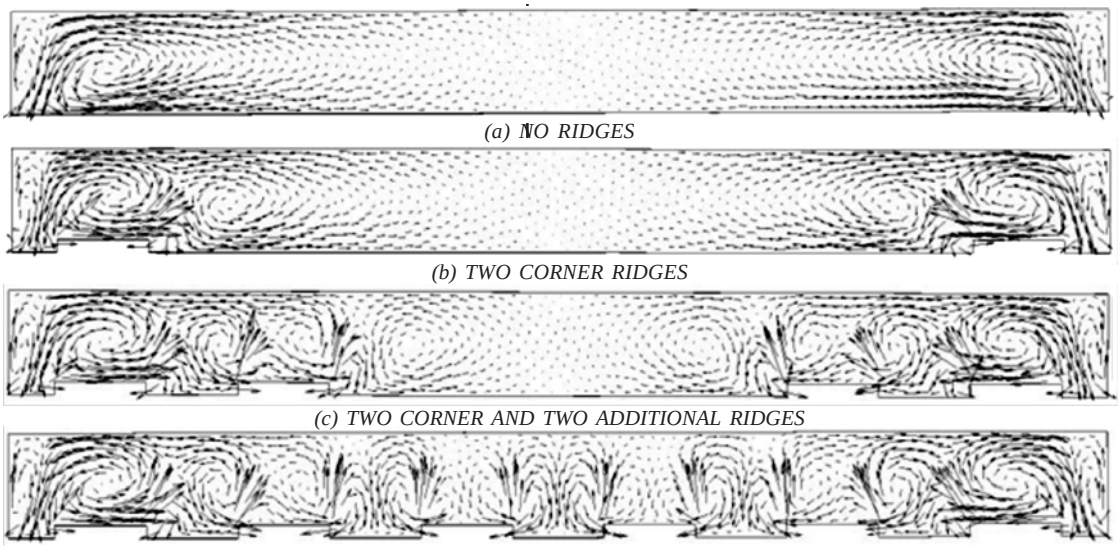

(a) NO RIDGES

(b) TWO CORNER RIDGES

(c) TWO CORNER AND TWO ADDITIONAL RIDGES

(d) TWO CORNER AND FOUR ADDITIONAL RIDGES

FIG. 3. VARIATION OF SECONDARY CURRENTS WITH DEVELOPMENT OF RIDGES

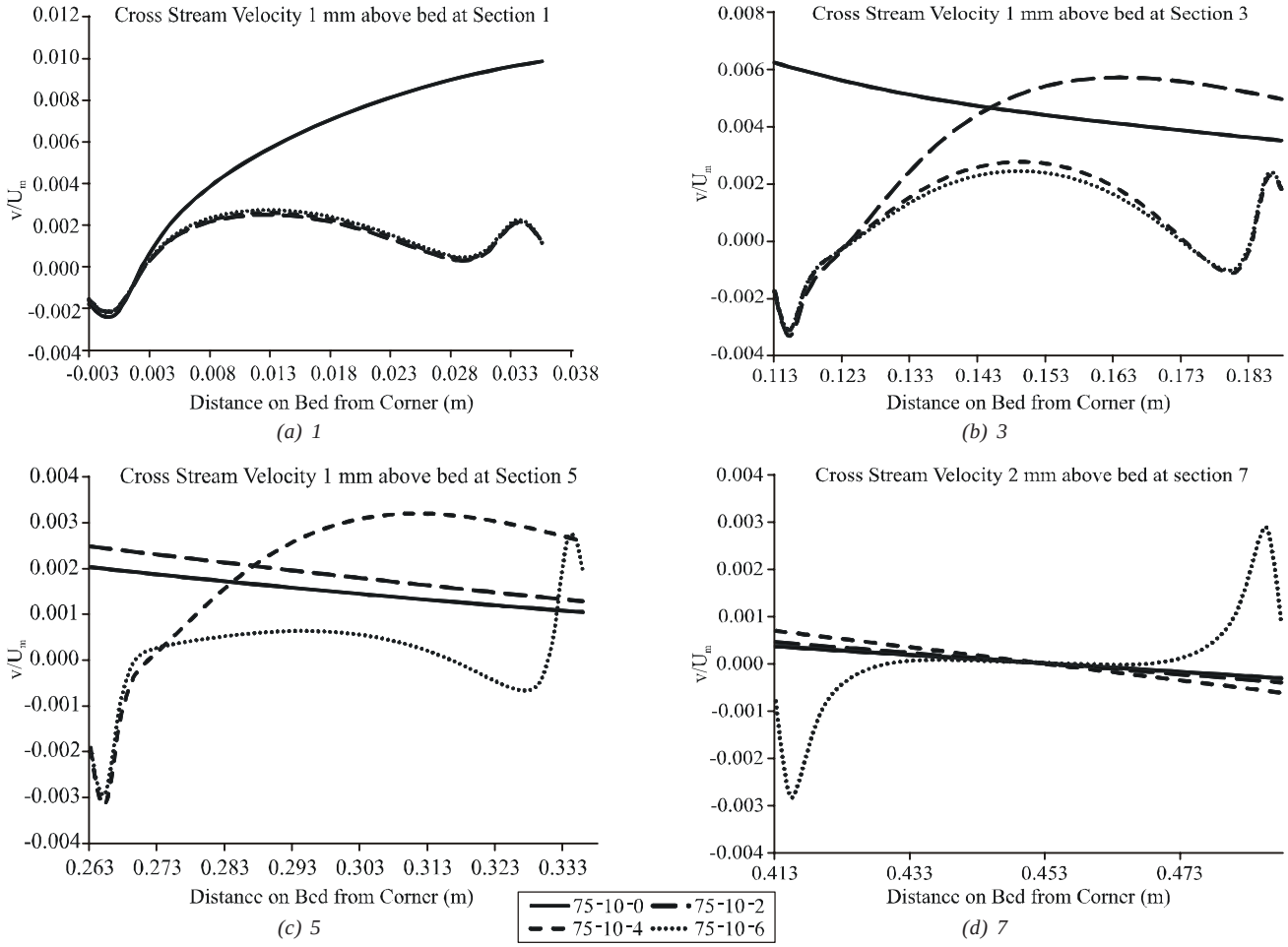

FIG. 4. VARIATION OF NON-DIMENSIONALIZED CROSS-STREAM VELOCITY, V/U_M, WITH RIDGE DEVELOPMENT AT LOCATIONS AS DEFINED IN FIG. 1

4.3 Variation of Wall Shear on the Bed

The non-dimensionalized wall shear, $\tau_{bx}/\rho ghS$ on the bed in the stream wise and cross stream directions is plotted for the Case 75-10-0 (i.e. the channel without the bed forms) and is shown in Fig. 5. The wall shear in the stream wise direction is seen to peak initially in the wall zone and then attains its maximum in the central portion of the channel. The peak in the wall zone could explain local scouring of the bed and ultimately the development of the first trough near the walls; the peak in the wall shear in the cross stream direction which is found to be around the same area could also be responsible for the shift of the scoured bed material towards one side and ultimately responsible for the creation of the first ridge near the walls, as was suggested by Nezu, et. al. [11].

Fig. 6 shows non-dimensionalized wall shear on the bed in the mainstream direction, with variation in the number of ridges, at four different Locations for Cases 75-10-0, 75-10-2, 75-10-4 and 75-10-6. The graph shows that wall shear at each location, i.e. Locations 1, 3, 5 and 7 (as defined in Fig. 1), is seen to be falling with the development of a ridge adjacent to the region it and remains at a similar lower value as other ridges appear.

Fig. 7 shows the non-dimensionalized wall shear on the bed in the cross-stream direction, $\tau by/\rho ghS$, with variation in the number of ridges, at four different Locations for Cases 75-10-0, 75-10-2, 75-10-4 and 75-10-6. The graph shows wall shear which is peaking only at Location 1 (as defined in Fig. 1) when there is no ridge, is found to be increasing with the development of a ridge adjacent (towards corner) to it and remains unchanged until the end of the ridge development.

These results suggest that one possible mechanism for the creation of ridges would be tied to secondary circulations, and wall shear on the bed in the wall zone. As the corner ridges form due to the corner vortex and peak wall shear in Location 1, the re-circulations would form and "propagate" towards the channel central line, which would then lead to formation of the next ridge(s) on the bed. As ridges appear they themselves are responsible for localised increase in velocity and shear again with the potential to erode material and reshape the bed. Eventually a trough-and-ridge bed would be formed across the channel bed section related to strong secondary currents activity, leading in turn to surface boils.

4.4 Variation of Wall Shear after Ridge Formation

Average shear stresses on the bed and sidewalls are calculated at every section of cross section as shown in Fig. 1 and are non-dimensionalized by ρghS. The results are tabulated in Table 2 for the Cases 75-10-0, 75-10-2, 75-10-4 and 75-10-6. The table clearly shows that the average shear stress in any section within the cross section of the channel keeps on decreasing with the development of the

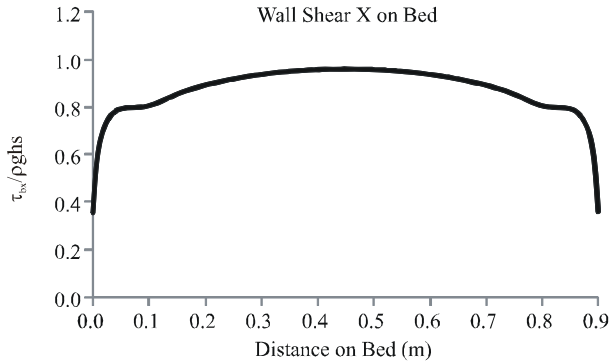

(a) FLOW DIRECTION

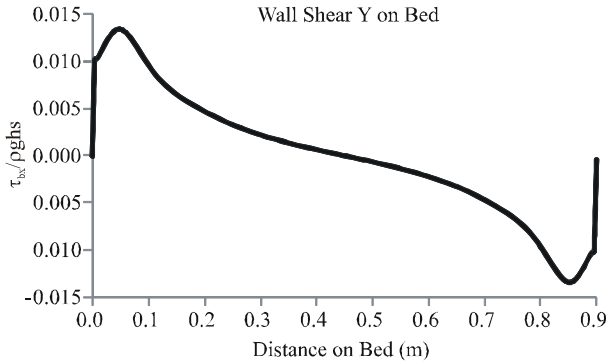

(b) CROSS-STREAM DIRECTION ON THE BED ACROSS THE WIDTH OF THE CHANNEL

FIG. 5. WALL SHEAR

ridges. This shows that a state of equilibrium may be reached on the channel boundaries as part of the interaction between bed form and currents (balance between secondary flow and bed response/form).

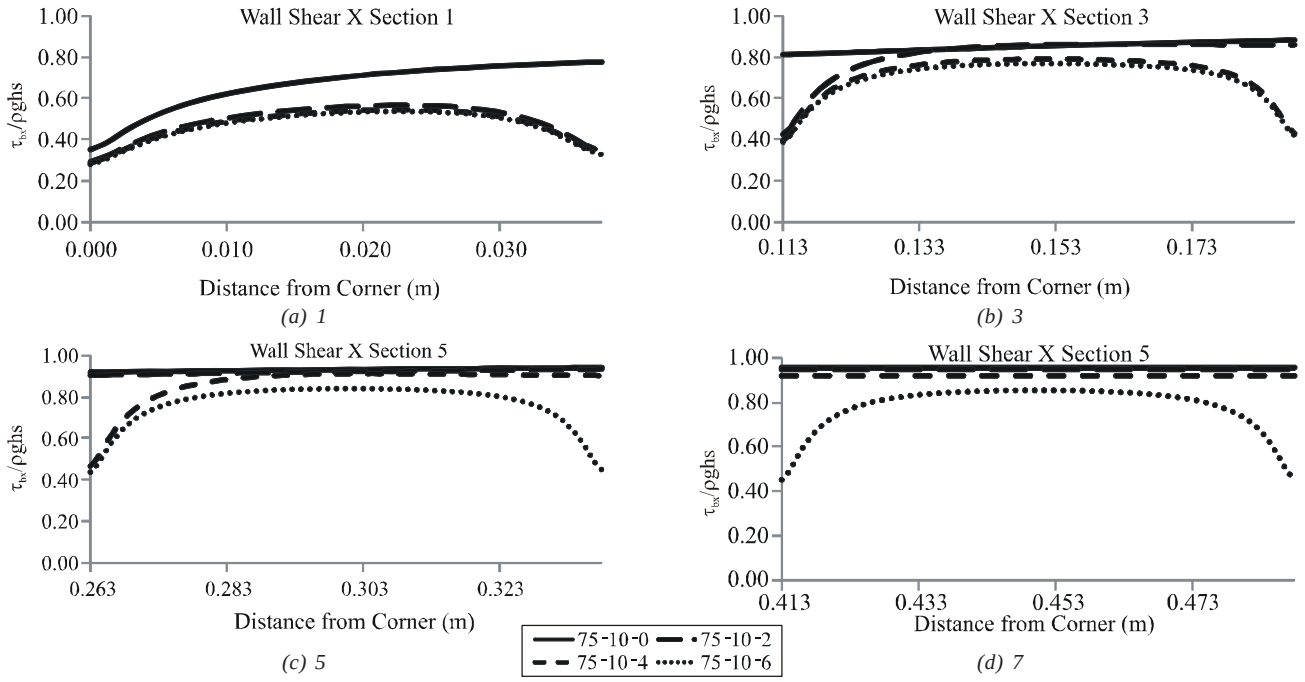

FIG. 6. VARIATION OF NON-DIMENSIONALIZED WALL SHEAR ON BED, $\tau_{bx}/\rho ghS$, IN MAINSTREAM DIRECTION WITH RIDGE DEVELOPMENT AT LOCATIONS (AS DEFINED IN FIG. 1)

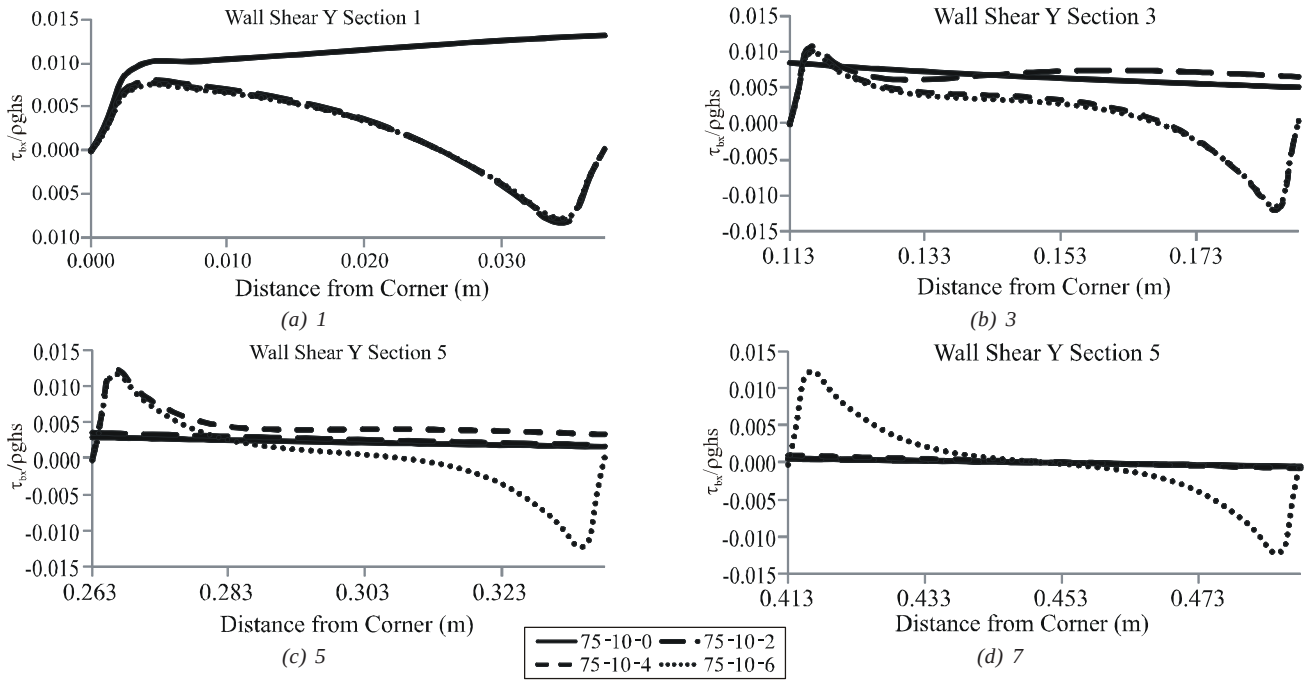

FIG. 7. VARIATION OF NON-DIMENSIONALIZED WALL SHEAR ON BED, $\tau_{bx}/\rho ghS$, IN CROSS-STREAM DIRECTION WITH RIDGE DEVELOPMENT AT LOCATIONS (AS DEFINED IN FIG. 1)

4.5 Isovel Pattern

Fig. 8 shows the isovel patterns plotted for the mainstream velocity for Case 75-10-6. They show a periodic variation in the cross-stream direction. A low speed zone is formed on the regions above the ridges while a higher speed zone is formed in the regions above the troughs.

The mainstream velocity is also plotted at different depths in the central and sidewall zones of the channel and is shown in Fig. 9. The results show high velocity flow over the troughs and comparatively low velocity flow over the ridges at the same distance from the bed. The difference of velocities is naturally higher near the ridges and goes on decreasing near the free surface. It can be noted that low speed and high speed streams of water flow side by side periodically throughout the width of the channel. These low speed streams have the potential to contain high sediment concentrations as has been reported by previous researchers such as Wang, et. al. [4].

4.6 Variation of Secondary Currents with Depth

Figs. 10-12 show the non-dimensionalised three components of the velocity u, v, and w plotted for the Case 75-10-6 at four different depths i.e. 15, 25, 45 and

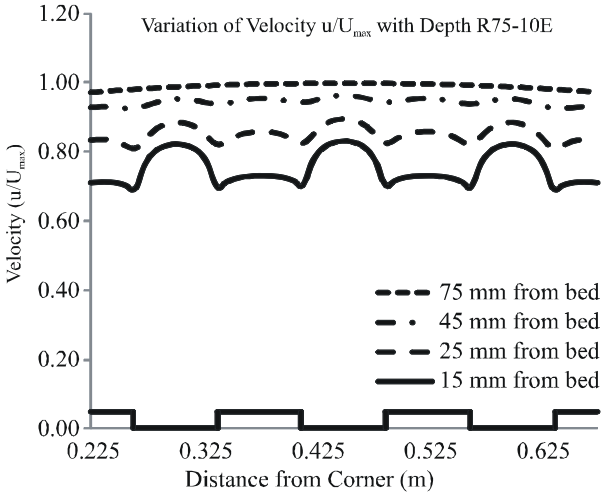

FIG. 9. VARIATION OF NON-DIMENSIONALIZED MAINSTREAM VELOCITY U/U$_{max}$ WITH DEPTH FOR CASE 75-10-6

TABLE 2. VARIATION OF WALL SHEAR ON BED AND SIDEWALL WITH RIDGE DEVELOPMENT.

Location	Shear stress $\tau_b/\rho ghS$			
	No Ridges	Two Ridges	Four Ridges	Six Sidges
Location 1	0.66220	0.49216	0.47338	0.46748
Location 2	0.79574	0.76812	0.72591	0.71251
Location 3	0.84892	0.81478	0.71828	0.69967
Location 4	0.90171	0.88136	0.85765	0.81695
Location 5	0.93317	0.91992	0.86387	0.76656
Location 6	0.95024	0.93996	0.90787	0.85799
Location 7	0.95560	0.94634	0.91845	0.78193
Left wall	0.70913	0.62894	0.60224	0.59396

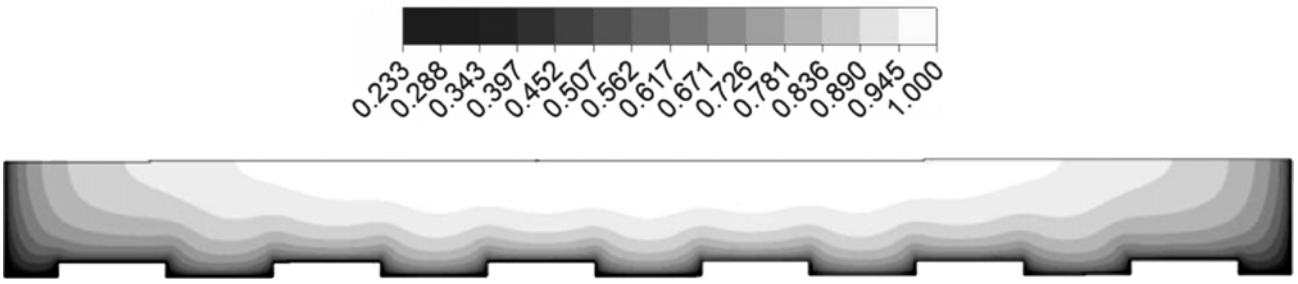

FIG. 8. PLOT OF THE ISOVELS FOR U/UMAX FOR CASE 75-10-6

75mm from the bed level. The mainstream velocity, u, is seen to be varying such that there is lower velocity over the ridges and comparatively higher velocity over the troughs. This difference is higher near the bed and goes on decreasing towards the free surface where almost the same velocity is observed throughout the central portion.

The cross stream velocity, v, is seen to have higher magnitudes over the troughs as compared to ridges as shown in Fig. 11. The magnitude of the velocity is greater near the bed and gets decreased in the central portion but is again found to increase near the free surface. The velocity is seen to change sign over the centres of both troughs and ridges and hence two cells (a pair) of counter rotating currents are formed over each section. Near the free surface the velocity only changes sign over the middle trough (Section 7, Fig. 1) of the channel which means that effect of the ridges is very negligible near the free surface and only two large counter rotating cells are seen on either side of the centre.

The vertical velocity, w, is taken positive upward and negative downward. It is seen to be highest in magnitude over the edges of the ridges. It is found to be positive over the areas where troughs and ridges meet and negative over the middle portions of both troughs and ridges as shown in Fig. 12. The upward velocities are higher in magnitude than the downward velocities. The downward velocity is higher over troughs as compared to ridges and hence may be responsible for the high sediment concentration over the ridges as seen previously. The vertical velocities are found to be higher near the bed and decrease near the free surface. The results for the other channels i.e. Cases 75-05-6 and 50-10-6 were also found to be similar in nature.

4.7 Sensitivity to Height of Ridge

Comparison of flow structures is done between Cases 75-10-6 and 75-05-6 to see the effect of the height of the ridge on the cellular secondary currents. The velocities are plotted at depths 15 mm and 10 mm from the bed for the two Cases 75-10-6 and 75-05-6 respectively, keeping an equal distance of 5mm from the top of the ridges and are shown in Fig. 13. Not much effect is seen on the mainstream velocity, u, with the variation in ridge height. However, in the cross stream velocity, v, it is found that two circulations are visible over the troughs as the velocity is changing sign but over the ridges it is seen to be going in one direction i.e. away from the wall for the

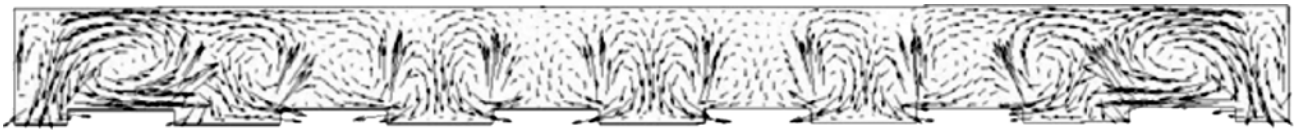

(a) 75-10-6

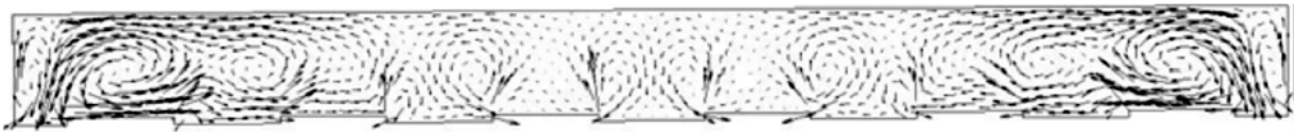

(b) 75-05-6

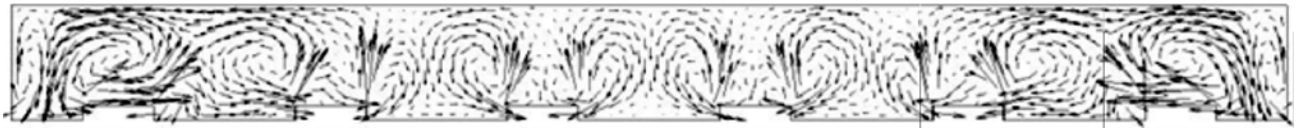

(c) 50-10-6

FIG. 10. VARIATION OF CELLULAR SECONDARY CURRENTS WITH SIZE OF RIDGES FOR CASES

Case 75-05-6; whereas, the flow seems to have fully developed when height of the ridge increases to 10mm, as two counter rotating circulations are visible on both troughs and ridges. The vertical velocity, w, is found to have the maximum difference, especially the upward velocity, and is seen to be directly proportional to the ridge height.

4.8 Sensitivity to Width of Ridge

Comparison of flow structures is done between Cases 75-10-6 and 50-10-6 to see the effect of the length of the ridge on the cellular secondary currents. The velocities are plotted at a depth of 15mm from the bed for Cases 75-10-6 and 50-10-6 respectively, as shown in Fig. 14. Again not much effect is seen on the mainstream velocity, u, and the cross stream velocity, v, with the variation in ridge length. The vertical velocity, w, is found to have the some difference here as well specially the upward velocity and is seen to increase further with the decrease in length of the ridge.

5. CONCLUSIONS

The pattern of the secondary currents as observed shows that the presence of the sidewalls could initially be responsible for the creation of the corner ridges. These, in turn, may be responsible for the formation of an additional cell of circulation which again creates another ridge and so on until the whole channel develops these ridges and troughs and a state of equilibrium is reached. This would provide an explanation for the mechanism leading to ridge formation and appearance of lines of boil, consistent with earlier hypotheses found in the

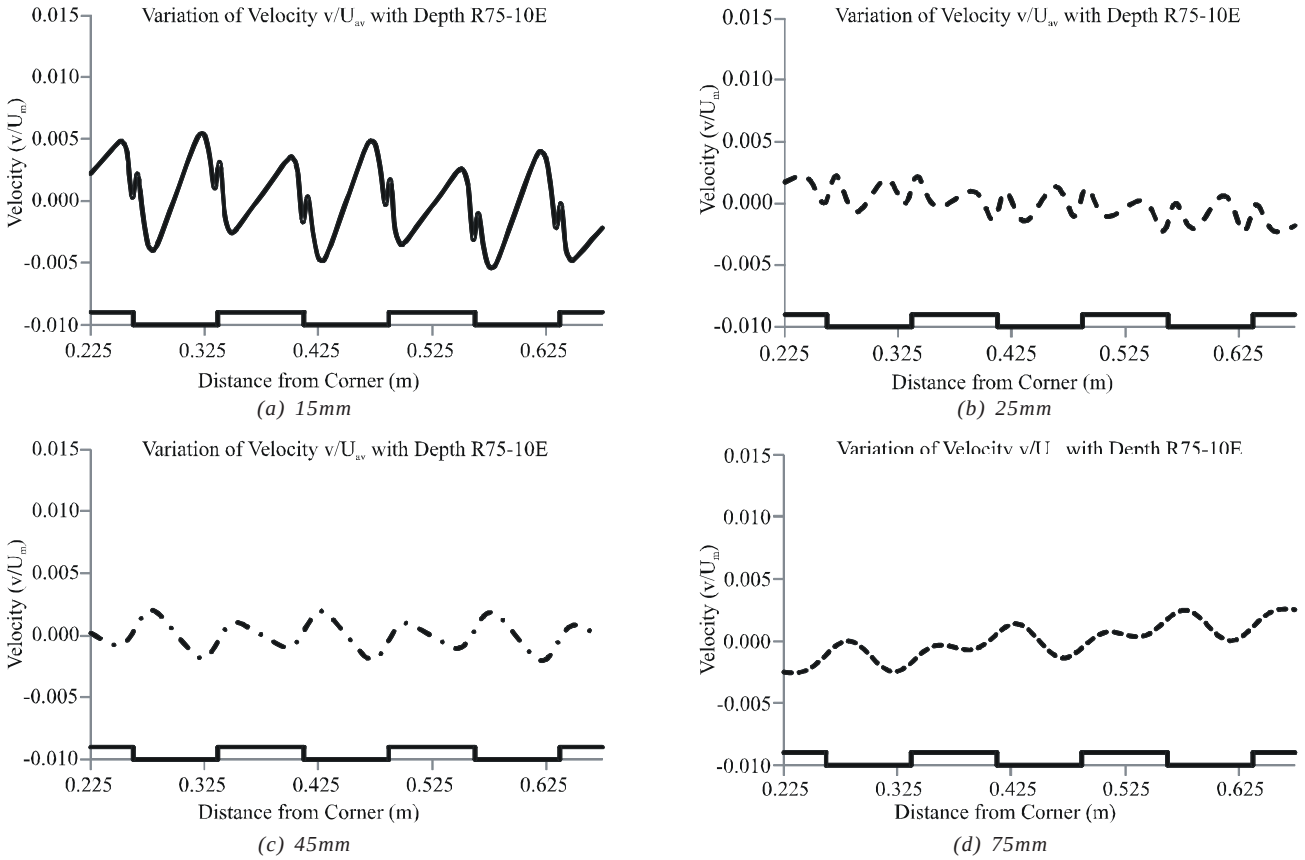

FIG. 11. VARIATION OF NON-DIMENSIONALIZED CROSS-STREAM VELOCITY, V/U$_m$, IN CENTRAL PORTION OF CHANNEL WITH DEPTH (FROM BED LEVEL, FOR THE CASE 75-10-6

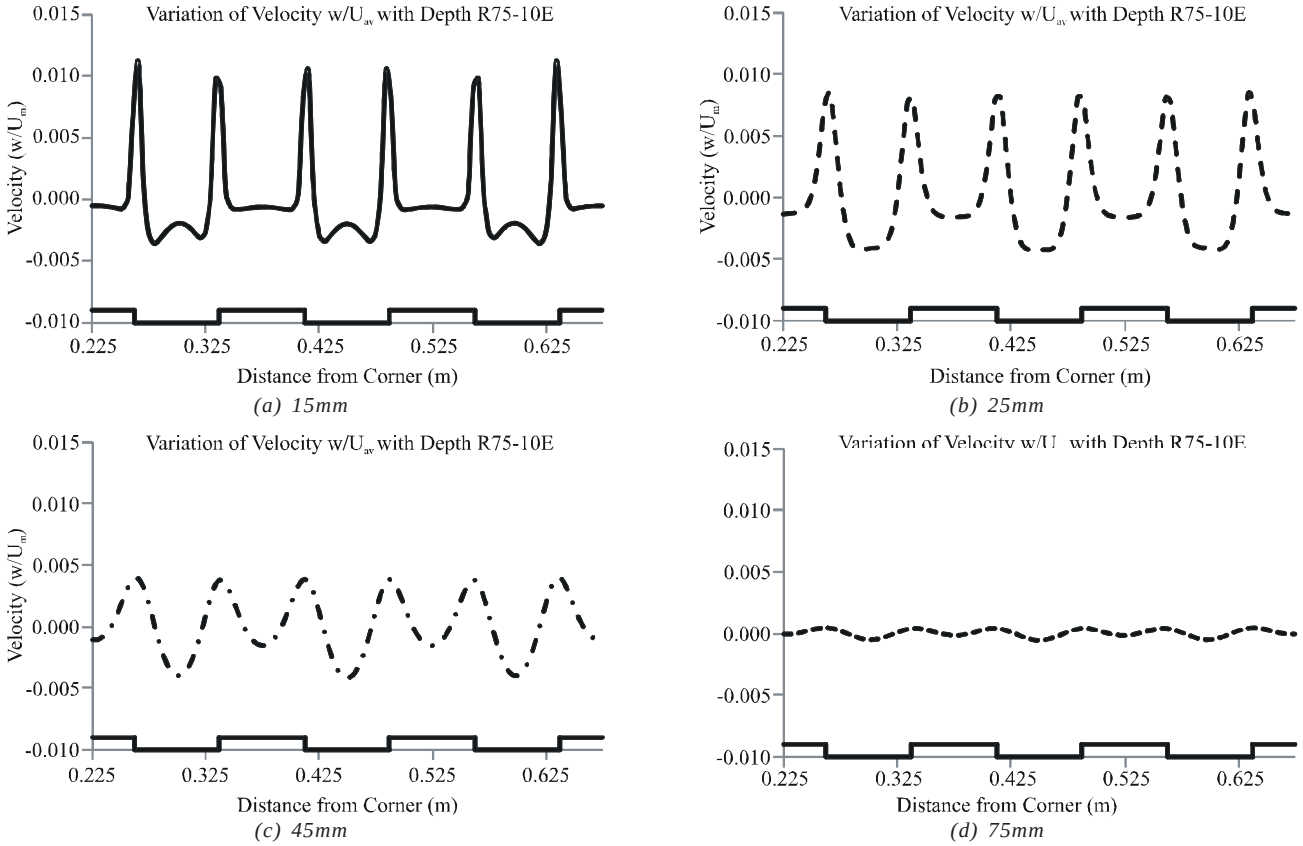

FIG. 12. VARIATION OF NON-DIMENSIONALIZED VERTICAL VELOCITY, W/U$_m$, IN CENTRAL PORTION OF CHANNEL WITH DEPTH FROM BED LEVEL, FOR THE CASE 75-10-6

literature. The vertical velocity is found to be upward over the edges of the ridges and downward over centres of both the troughs and ridges, which shows a pair of counter rotating cells over both troughs and ridges. The perturbations of secondary flow are strong near the bed and get significantly reduced near the free surface. The wall shear is seen to be decreasing with the increase in the ridges on the bed which shows that the bed forms ultimately bring some stability on the boundaries in the section.

ACKNOWLEDGEMENTS

The first author is very grateful to Mehran University of Engineering & Technology, Jamshoro, Pakistan, for providing funds to conduct this research at University of Nottingham, UK.

REFERENCES

[1] Nezu, I., and Rodi, W., "Experimental Study on Secondary Currents in Open Channel Flow", 21st IAHR Congress, pp. 115-119, Melbourne, Australia, 1985.

[2] Prandtl, L., "Essentials of Fluid Dynamics: With Applications to Hydraulics, Aeronautics, Meteorology and other Subjects (English Translation)", Blackie and Son Ltd., pp. 145-149, 1952.

[3] Wang, Z.Q., and Cheng, N.S., "Secondary Flows Over Artificial Bed Strips", Advances in Water Resources, Volume 28, pp. 441-450, USA, 2005.

[4] Wang, Z.Q., and Cheng, N.S., "Time-Mean Structure of Secondary Flows in Open Channel with Longitudinal Bed Forms", Advances in Water Resources, Volume 29, pp. 1634-1649, USA, 2006.

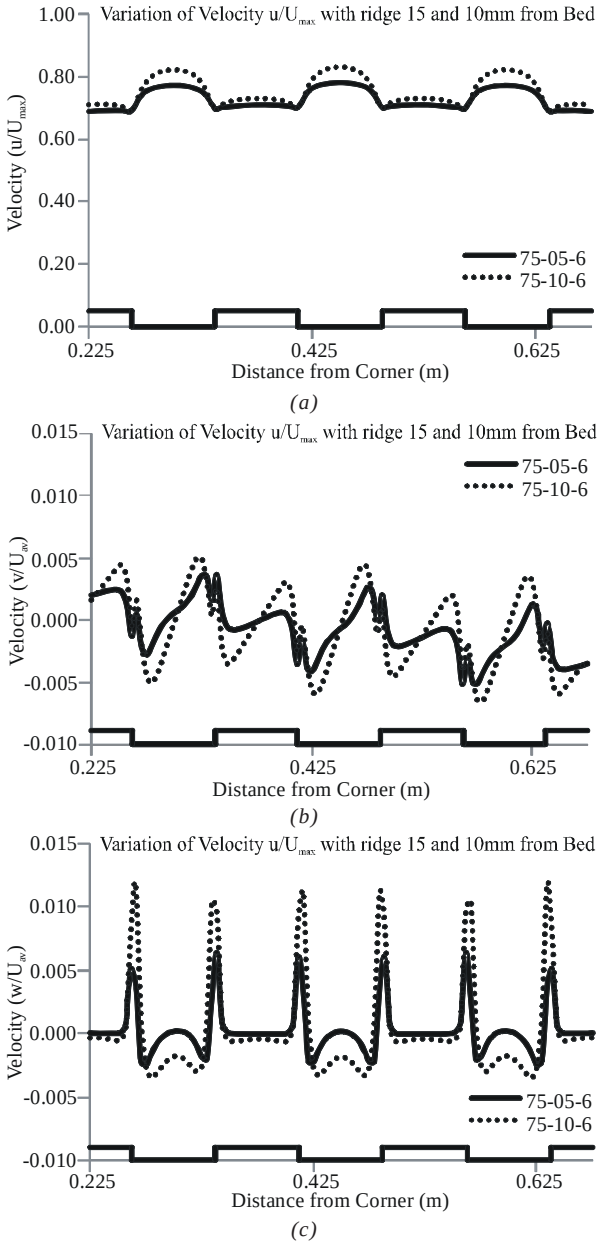

FIG. 13. VARIATION OF VELOCITY WITH RIDGE HEIGHT AT 5mm FROM RIDGE TOP

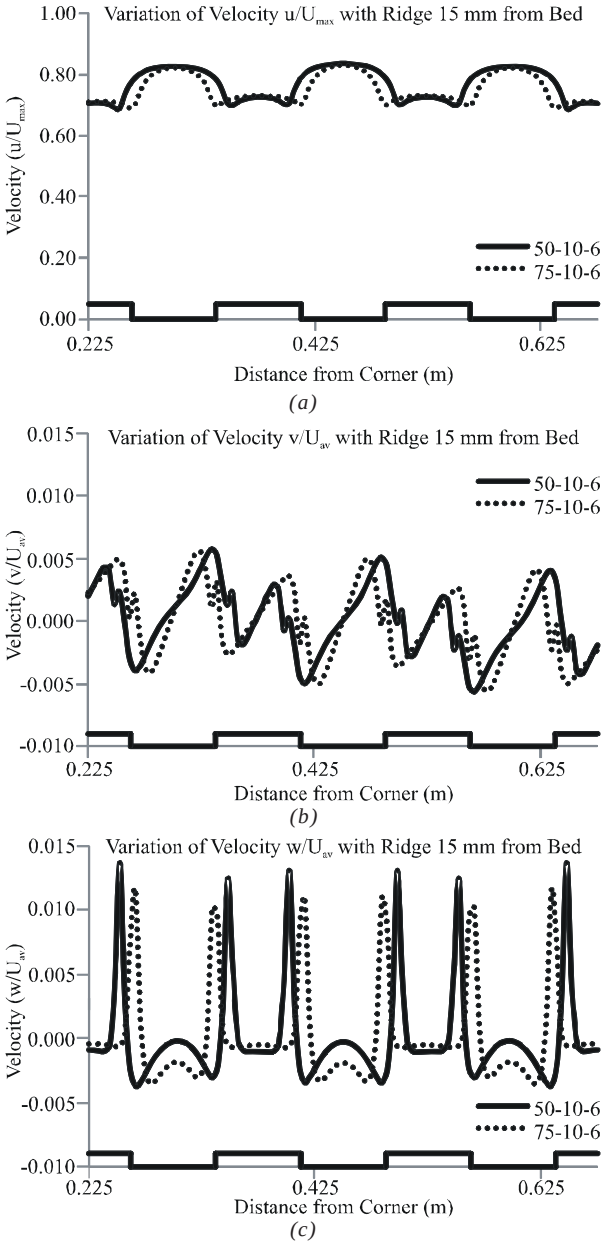

FIG. 14. VARIATION OF VELOCITY WITH RIDGE WIDTH AT 15mm FROM BED LEVEL

[5] Nezu, I., "Open-Channel Flow Turbulence and its Research in 21st century", Journal of Hydraulic Engineering, ASCE, Volume 131, No. 4, pp. 229-246, USA, 2005.

[6] Nezu, I., and Nakagawa, H., "Cellular Secondary Currents in Straight Conduits", Journal of Hydraulic Engineering, ASCE, Volume 110, No. 2, pp. 173-193, USA, 1984.

[7] Nezu, I., Nakagawa, H., and Kawashima, N., "Cellular Secondary Currents and Sand Ribbons in Fluvial Channel Flows", 6th Congress, Asian and Pacific Regional Division, IAHR, pp. 51-58, Kyoto, Japan, 1988.

[8] Nezu, I., and Nakagawa, H., "Self Forming Mechanism of of Longitudinal Sand Ridges and Troughs", Proceedings of 23rd IAHR Congress, Volume B, IAHR, pp. 65-72, Delft, The Netherlands, 1989.

[9] Nezu, I., and Nakagawa, H., "Turbulence in Open-Channel Flows", IAHR-Monograph, Balkema, Rotterdam, The Netherlands, 1993.

[10] Colombini, M., "Turbulence-Driven Secondary Flows and Formation of Sand Ridges", Journal of Fluid Mechanics, Volume 254, pp. 701-719, UK, 1993.

[11] Ikeda, S., "Self-Formed Straight Channels in Sandy Beds", Proceedings of ASCE, Journal of Hydraulic Division, Volume 107, No. 4, pp. 389-406, USA, 1981.

[12] Nezu, I., Nakagawa, H., and Tominaga, A., "Secondary Currents in a Straight Channel Flow and Relation to its Aspect Ratio", Turbulent Shear Flows 4, Volume 4, Springer, pp. 246-260, New York, USA, 1985.

[13] Ansari, K., Morvan, H.P., and Hargreaves, D.M., "A Numerical Investigation into Secondary Currents and Wall Shear in Trapezoidal Channels", Journal of Hydraulic Engineering, ASCE, Volume 137, No. 4, pp. 432-440, USA, 2011.

[14] Choi, S.U., Park, M., and Kang, H., "Numerical Simulations of Cellular Secondary Currents and Suspended Sediment Transport in Open-Channel Flows Over Smooth-Rough Bed Strips", Journal of Hydraulic Research, Volume 45, No. 6, pp. 829-840, UK, 2007.

[15] Ansys, Inc., Ansys-CFX, Version 11.0 Southpointe, 275, Technology Drive, Canonsburg, PA, USA, 2008.

[16] Cokljat, D., "Turbulence Models for Non-Circular Ducts and Channels", Ph.D. Thesis, Department of Civil Engineering, City University, London, England, 1993.

[17] Launder, B.E., Reece, G.J., and Rodi, W., "Progress in the Developments of a Reynolds-Stress Turbulence Closure", Journal of Fluid Mechanics, Volume 68, pp. 537-566, UK, 1975.

[18] Speziale, C.G., Sarkar, S., and Gatski, T.B., "Modelling the Pressure-Strain Correlation of Turbulence: An Invariant Dynamical Systems Approach", Journal of Fluid Mechanics, Volume 227, pp. 245-272, UK, 1991.

[19] Cacqueray, N.D., Hargreaves, D.M., and Morvan, H.P., "A Computational Study of Shear Stress in Smooth Rectangular Channels", Journal of Hydraulic Research, Volume 47, No. 1, pp. 50-57, UK, 2009.